

11. E. Ruckenstein, A. S. Vaidyanathan, and G. R. Joungaeist, Chem. Eng. Sci., 26, 1305 (1971).
12. L. P. Zolotarev and M. I. Dubinin, Izv. Akad. Nauk SSSR, Ser. Khim., 136 (1973).
13. I. N. Bekman and A. P. Brovko, Radiokhimiya, 23, No. 2, 275 (1981).

EXPERIMENTAL METHODS FOR STUDYING THE DIFFUSION OF RADIOACTIVE
GASES IN SOLIDS.

VIII. LONGITUDINAL-SECTION METHOD

I. N. Bekman, I. M. Buntseva,
and A. A. Shvyryaev

UDC 539.16.07:532.72:678.742

The methodical details of the application of the longitudinal-section method in combination with autoradiography to the study of the diffusion of radioactive gases and vapors in solids have been considered. The diffusion parameters of cyclohexane, carbon tetrachloride, and benzene labeled with carbon-14 in low-density polyethylene have been determined. Various mathematical models of the diffusion of vapors in polymers, viz., classical diffusion, diffusion in the presence of radioactive decay or a first-order chemical reaction, diffusion with trapping, dissociative diffusion, and diffusion with concentration and coordinate dependences of the diffusion coefficient, have been analyzed. A method for treating experimental data has been proposed. Concentration dependences of the diffusion coefficient have been calculated from the distribution curves of the concentration across the thickness of the sample. It has been shown that the plasticizing effect of the diffusates becomes stronger along the series: cyclohexane, carbon tetrachloride, benzene.

The longitudinal-section method has become widely used in the study of the migration of impurities in solids. Its main advantage is the possibility of the direct monitoring of the development of the diffusion process in the sample. Anomalies of various kinds associated with the concentration, coordinate, and time dependence of the diffusion coefficient can be detected and interpreted by just this method.

In the present communication we shall examine the features of the use of the longitudinal section method in combination with the autoradiographic monitoring of the distribution of an impurity in a sample to study the migration of gaseous and vapor impurities labeled by a radioactive isotope. The proposed methods were tested in the example case of the diffusion of vapors of organic compounds, viz., cyclohexane, carbon tetrachloride, and benzene labeled with carbon-14, in low-density polyethylene of type 102-03003. The samples were blocks with a 10 × 10 mm cross section cut from a single plate, which was obtained by molding from a melt. The measurement of the diffusion coefficients of the labeled substance was carried out both in the dry polymer and in the polymer preliminarily saturated with vapors of the same, but inactive diffusate.

The apparatus (Fig. 1) consisted of a glass vessel, in whose central part were placed the samples, and test tubes with the diffusate. The sorption vessel and the test tube were fitted with their own thermostating jackets, which made it possible to study the diffusion of the vapors at various partial pressures. The working temperature range was 20-150°C. As a rule, the diffusion annealing was carried out in an atmosphere of saturated vapors of the diffusate. The diffusion time corresponded to fulfillment of the conditions of a semi-infinite medium. At the conclusion of an experiment, the samples were suddenly cooled in vapors of liquid nitrogen. Then with the aid of a microtome, a section was cut from the sample in the direction of the passage of the diffusing substance. The total amount of absorbed radioactive impurity was determined by an end-window β counter. The longitudinal sections were brought into contact with a nuclear photographic emulsion. The exposure was carried out in a cooling chamber.

Translated from Radiokhimiya, Vol. 25, No. 2, pp. 261-268, March-April, 1983. Original article submitted April 20, 1982.

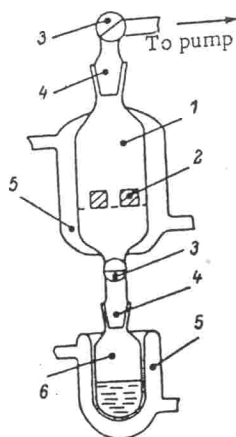


Fig. 1

Fig. 1. Schematic representation of the apparatus for carrying out the sorption experiments: 1) sorption vessel; 2) polyethylene samples; 3) vacuum valves; 4) ground-glass joints; 5) thermostating jackets; 6) vessel with radioactive liquid.

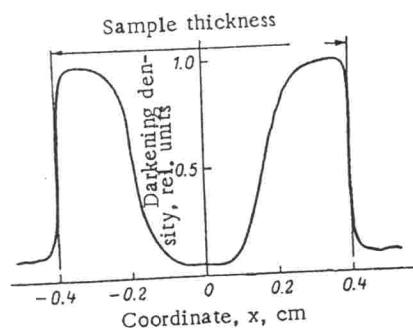


Fig. 2

Fig. 2. Typical photometric curve of an autoradiogram for the diffusion of organic solvents labeled with carbon-14 in polyethylene.

with a temperature of -20°C . It was shown by special experiments that no appreciable migration of the impurity through the sample occurs during all the operations after the conclusion of the diffusion experiment.

The developed autoradiograms were subjected to photometric measurement along the diffusion front by a type MF-4 microphotometer, which was subjected to significant modernization: The photographic paper was replaced by an electronic recording system, a photoresistor serving as the light detector. The signal from the photoresistor was converted into a series of rectangular pulses, whose frequency was proportional to the intensity of the light. The pulsed signal was fed simultaneously into the device for measuring the counting rate, which was connected to an electronic potentiometer (making it possible to directly record the blackening density-distance curve), and into a scaler, which was connected to a numerical printer (making it possible to obtain the information in the form of numerical fields, which were then fed into a computer for treatment of the results).

The analysis of the autoradiograms for the diffusion systems studied showed that the distribution of the diffusing impurity has a step character, the photometric curve (Fig. 2) being convex relative to the coordinate axis. In order to interpret the results obtained, let us consider various models of the diffusion of low-molecular-weight impurities in polymers.

In the framework of classical diffusion, the distribution of the concentration from a constant source into a plate of thickness H (under boundary conditions of the first kind on both surfaces of the plate) is described by the equation [1]

$$\frac{C(x, t)}{C_0} = \sum_{n=1}^{\infty} (-1)^{n+1} \left\{ \operatorname{erfc} \frac{(2n-1) - \frac{2x}{H}}{2\sqrt{u}} + \operatorname{erfc} \frac{(2n-1) + \frac{2x}{H}}{2\sqrt{u}} \right\} =$$

$$= 1 - \frac{4}{\pi} \sum_{m=0}^{\infty} \frac{1}{2m+1} \exp \{ -(2m+1)^2 \pi^2 u \} \sin \frac{(2m+1)\pi}{H} x,$$

where $u = Dt/H^2$, D is the diffusion coefficient, t is the diffusion time, C_0 is the concentration on the exit surface of the membrane, and x is the coordinate. Here the series on the left-hand side of the equation converges rapidly at short times, and the series on the right-hand side converges rapidly at long times.

In the case of diffusion in a semi-infinite body, the distribution of the concentration has the form

$$C(x, t) = C_0 \left(1 - \operatorname{erf} \frac{x}{2\sqrt{Dt}} \right). \quad (2)$$

If the diffusing impurity undergoes radioactive decay with a decay constant λ , we have [2]

$$C = C_0 \left(1 - \sum_{\nu=0}^{\infty} f(x) \frac{\lambda + \nu \exp[-(\lambda + \nu)t]}{\lambda + \nu} \right),$$

where

$$f(x) = \frac{4}{\pi} \sum_{m=0}^{\infty} \frac{(-1)^m}{(2m+1)} \cos \frac{(2m+1)\pi x}{H}; \quad \nu = \frac{\pi^2 D (2m+1)^2}{H^2}. \quad (3)$$

In the case of diffusion in a semi-infinite medium [3],

$$C = C_0 \left[\frac{1}{2} \exp\left(-x\sqrt{\frac{\lambda}{D}}\right) \operatorname{erfc}\left(\frac{x}{2\sqrt{Dt}} - \sqrt{\lambda t}\right) + \frac{1}{2} \exp\left(-x\sqrt{\frac{\lambda}{D}}\right) \operatorname{erfc}\left(\frac{x}{2\sqrt{Dt}} + \sqrt{\lambda t}\right) \right], \quad (4)$$

where

$$\operatorname{erfc} Z = 1 - \operatorname{erf} Z = 1 - \frac{2}{\sqrt{\pi}} \int_0^Z e^{-y^2} dy.$$

From expression (4) it is clear that an exponential distribution of the concentration is established in the sample after long diffusion times:

$$C = C_0 \exp\left(-x\sqrt{\frac{\lambda}{D}}\right). \quad (5)$$

We consider so-called diffusion with trapping [4], i.e., the case in which the diffusing impurity is captured by traps and removed from the diffusion process for a certain time. In this case, the distribution of the concentration of the mobile form $C(x, t)$ and of the immobile form $m(x, t)$ is described by the expressions

$$C(x, t) = C_0 \left\{ 1 - \frac{2}{\pi} \sum_{m=0}^{\infty} \frac{1}{(2m+1)H} [(-a_1 + k_1 + k_2)t^{-a_1 t} + (a_2 - k_1 - k_2)e^{-a_2 t}] \sin \frac{(2m+1)\pi}{H} x \right\}, \quad (6)$$

$$m(x, t) = m_0 \left\{ 1 - \frac{2}{\pi} \sum_{m=0}^{\infty} \frac{1}{(2m+1)H} (a_2 e^{-a_1 t} - a_1 e^{-a_2 t}) \sin \frac{(2m+1)\pi}{H} x \right\},$$

where k_1 is the rate constant for capture of an atom by a trap, k_2 is the rate constant for the release of an atom from a trap,

$$a_1 = \frac{1}{2}(k_1 + k_2 + D\omega^2) - A; \quad a_2 = \frac{1}{2}(k_1 + k_2 + D\omega^2) + A;$$

$$A = \sqrt{k_1 k_2 + \frac{1}{4}(k_1 - k_2 + D\omega^2)^2}; \quad \omega = \frac{(2m+1)\pi}{H}.$$

In the case of dissociative diffusion [5], i.e., in the case of diffusion along two channels between which an interaction formally described by a reversible first-order chemical reaction, we obtained the following expressions:

$$C_1 = C_1^\infty + \sum_{m=0}^{\infty} (A_1 e^{-a_1 t} + A_2 e^{-a_2 t}) \sin \omega x, \quad (7)$$

$$C_2 = C_2^\infty + \sum_{m=0}^{\infty} (A_3 e^{-a_1 t} + A_4 e^{-a_2 t}) \sin \omega x.$$

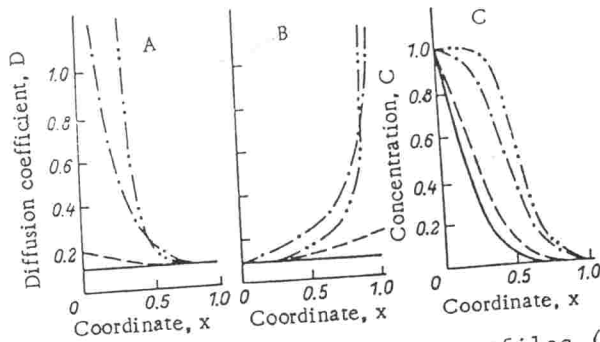


Fig. 3. Calculated concentration profiles (C) for various types of dependences of the diffusion coefficients on the concentration (B) and on the coordinate (A).

here

$$\begin{aligned}
 C_1^\infty &= \frac{(C_1^0 D_1 + C_2^0 D_2) k_2}{D_1 k_2 + D_2 k_1} + \frac{(k_1 C_1^0 + k_2 C_2^0) D_2}{D_1 k_2 + D_2 k_1} \left[\frac{\text{sh } zx + \text{sh } z(H-x)}{\text{sh } zH} \right]; \\
 C_2^\infty &= \frac{k_1 (C_2^0 D_2 + C_1^0 D_1)}{D_1 k_2 + D_2 k_1} - \frac{(k_1 C_1^0 - k_2 C_2^0) D_1}{D_1 k_2 + D_2 k_1} \left[\frac{\text{sh } zx + \text{sh } z(H-x)}{\text{sh } zH} \right]; \\
 A_1 &= \frac{\Psi_1 (-\alpha_1 + D_2 \omega^2 + k_2) + k_2 \Psi_2}{2A}; \quad A_2 = \frac{\Psi_1 (\alpha_2 - D_2 \omega^2 - k_2) - k_2 \Psi_2}{2A}; \\
 A_3 &= \frac{\Psi_2 (-\alpha_1 + D_1 \omega^2 + k_1) + k_1 \Psi_1}{2A}; \quad A_4 = \frac{\Psi_2 (\alpha_2 - D_1 \omega^2 - k_1) - k_1 \Psi_1}{2A}; \\
 \Psi_1 &= \frac{4}{H\omega} \left[-\frac{k_2 (C_1^0 D_1 + C_2^0 D_2)}{D_1 k_2 + D_2 k_1} - \frac{4\omega (k_1 C_1^0 - k_2 C_2^0) D_2}{(z^2 + \omega^2) H (D_1 k_2 + D_2 k_1)} \right]; \quad z = \sqrt{\frac{k_1}{D_1} + \frac{k_2}{D_2}}; \\
 \Psi_2 &= \frac{4}{H\omega} \left[-\frac{k_1 (C_2^0 D_1 + C_1^0 D_2)}{D_2 k_1 + D_1 k_2} + \frac{4\omega (k_1 C_1^0 - k_2 C_2^0) D_1}{(z^2 + \omega^2) H (D_2 k_1 + D_1 k_2)} \right]; \quad \omega = \frac{(2m+1)\pi}{H}; \\
 \alpha_1 &= \frac{1}{2} [(D_1 + D_2) \omega^2 + k_1 + k_2] - A; \\
 \alpha_2 &= \frac{1}{2} [D_1 + D_2) \omega^2 + k_1 + k_2] + A; \\
 A &= \frac{1}{2} \sqrt{D_1 - D_2)^2 \omega^4 + 2(D_1 - D_2)(k_1 - k_2) \omega^2 + (k_1 + k_2)^2}.
 \end{aligned}$$

Here D_1 and D_2 are the diffusion coefficients along channels 1 and 2, respectively; k_1 is the probability of a transition from channel 1 to channel 2; k_2 is the probability of the reverse transition. When there is local equilibrium ($k_1 C_1^0 = k_2 C_2^0$), $C_1^\infty = C_1^0$, $C_2^\infty = C_2^0$;

$$\psi_1 = \frac{4}{H\omega} \left[-\frac{k_2 (C_1^0 D_1 + C_2^0 D_2)}{D_1 k_2 + D_2 k_1} \right]; \quad \psi_2 = \frac{4}{H\omega} \left[-\frac{k_2 (C_2^0 D_1 + C_1^0 D_2)}{D_2 k_1 + D_1 k_2} \right].$$

When $k_1 = 0$ and $k_2 = 0$, system (7) is transformed into expressions for parallel diffusion along two independent channels.

If the diffusion coefficient is dependent on the concentration, the equation for Fick's second law has the form [6]

$$\frac{\partial C}{\partial t} = \frac{\partial}{\partial x} \left[D(C) \frac{\partial C}{\partial x} \right] = D(C) \frac{\partial^2 C}{\partial x^2} + \left(\frac{\partial D(C)}{\partial C} \right) \left(\frac{\partial C}{\partial x} \right)^2. \quad (8)$$

This equation is nonlinear and, as a rule, does not have an analytical solution. However, if we take advantage of Boltzmann's substitution $\eta = x/\sqrt{t}$, then in the case of diffusion from a constant source into a semi-infinite medium, the concentration distribution is described by the expression

$$C(x, t) = C_0 \left(1 - \frac{\int_0^x B(x) e^{-\frac{1}{2t} \int_0^x B(x) x dx} dx}{\int_0^\infty B(x) e^{-\frac{1}{2t} \int_0^x B(x) x dx} dx} \right), \quad (9)$$

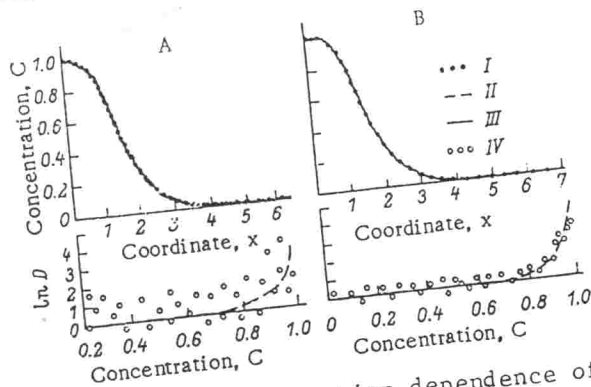


Fig. 4. Plots of the concentration dependence of the diffusion coefficient calculated from the concentration profile by the Matano-Boltzmann method: I) true concentration distribution; II) corresponding concentration dependence of the diffusion coefficient; III) concentration distribution with the imposition of a 3% statistical error (A) and after smoothing of the concentration curve by the spline method (B); IV) results of the calculation of $D(C)$ according to the Matano-Boltzmann method.

where $D = D[C(x)] = 1/B(x)$.

The problem of $D(C)$ is closely related to the problem of $D(x)$. In fact, as we see from Fig. 3, for a certain function $D(C)$ we can always find a $D(x)$ for which the concentration profile will be exactly the same as in the former case. It is impossible to distinguish these two cases on the basis of the data from one experiment. Experiments with different diffusion times are usually carried out and the functions $D(C)$ are formally calculated each time to discriminate between the models. If $D(C)$ is not dependent on the diffusion time, there is no coordinate dependence of the diffusion coefficient. (A debate on this question was presented in [7] and [8].)

From Fig. 3 it follows that the plots of $C(x)$ will be convex for a descending $D(x)$ and an ascending $D(C)$. We note that for the appearance of a flat area on the initial section of the concentration profile it is necessary for the function $D(C)$ to increase more rapidly than a simple exponential function.

We carried out detailed calculations according to all the diffusion models considered above. It was found that in the case of parallel diffusion there is a possibility of the appearance of concentration profiles characterized by the presence of deeply penetrating "tails" (discontinuities are observed on the straight lines when they are plotted in the linearized scale). Conversely, the presence of trapping results in narrowing of the concentration profile. Convex curves appear only in the case of concentration and coordinate dependences of the diffusion coefficient, as well as in certain special cases of dissociative diffusion (if local equilibrium is absent). In our experiments the diffusion times were sufficiently long for local equilibrium to be established; therefore, the model of dissociative diffusion may be discarded. The functions $D(C)$ calculated from the experimental data recorded after various diffusion times were identical. Therefore, the coordinate dependence of the diffusion coefficient may be neglected. Thus, the main reason for convex concentration profiles in the present case is the concentration dependence of the diffusion coefficient.

An algorithm for treating the results can be based on the numerical solution of Eq. (8) followed by the determination of the parameters of the concentration dependence of the diffusion coefficient. A shortcoming of such an approach is the *a priori* introduction of a concrete dependence for $D(C)$ [as a rule, in the form of $D = D(0)e^{\beta C}$], while the discovery of a dependence is the purpose of the work. Therefore, the treatment of the experimental data carried out by the Matano-Boltzmann method [9]. According to this method, in the case of diffusion from a constant source into a semi-infinite body, the diffusion coefficient at point C_1 on the concentration distribution curve can be found from the formula

$$D(C_1) = -\frac{1}{2t} \left(\frac{\partial x}{\partial C} \right)_{C_1} \int_0^{C_1} x dC.$$

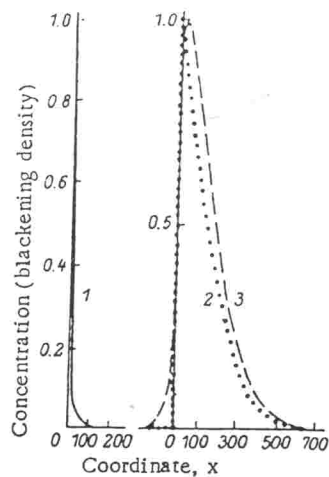


Fig. 5

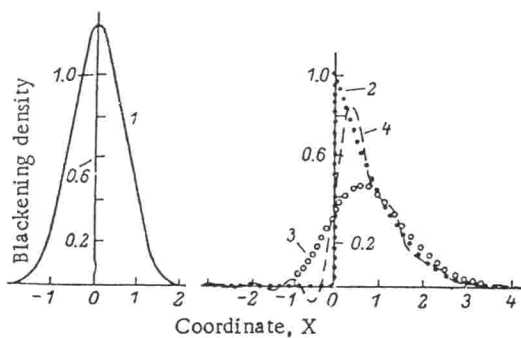


Fig. 6

Fig. 5. Distortion of the concentration distribution curve due to the presence of a free path for the radiation in the case of autoradiographic detection. 1) Distribution of the blackening concentration from an infinitely thin source in polyethylene; 2) true concentration distribution; 3) distorted concentration distribution curve.

Fig. 6. Reconstruction of a concentration distribution curve in the case of strong distortion (a large width of the response function): 1) response function; 2) true concentration distribution; 3) distorted concentration distribution curve; 4) curve obtained from reconstruction.

Then the problem of treating the results reduces to finding the derivative at the point C_i , i.e., $(\partial C/\partial x)_{C_i}$, and the integral, i.e., $\int_0^{C_i} x(C) dC$. The principle of the method is simple, but it is necessary to deal with considerable difficulties in its practical realization.

1. Since the calculations include graphical integration, the selection of the spacing with respect to the concentration and the integration method is a serious problem. The computational operations are tedious and require the use of a high-speed computer. The accuracy of the determination of D , especially in the extreme composition regions, is low. These difficulties were thoroughly analyzed in [10] and will not be considered here in detail.

2. While the integration process is a proper problem, the differentiation is classified as an improperly formulated problem in mathematical physics. In practice this means that the solution becomes unstable in the presence of statistical errors. The difficulties which arise in this case are illustrated in Fig. 4A, in which the results of model calculations have been presented. During the simulation, $D(C)$ was first assigned, and it was used to find the profile of $C(x)$, on which random errors of various magnitude were imposed. The testing of the program according to the Matano-Boltzmann method on this "experimental" file showed that the calculated values fluctuate strongly and that the dependence of $D(C)$ obtained has practically nothing in common with the original. In order to overcome this difficulty, the photometric curve was subjected to smoothing by the spline method. The conditions of the program were finalized with the aid of mathematical simulation. Figure 4B shows that the proposed methods make it possible to find an adequate functional dependence for $D(C)$.

3. The transition from the measured blackening density of the autoradiograph to the concentration profile presents a serious problem. In fact, the existence of a free path for the radiation, the finite thickness of the sample and the photographic emulsion, and so forth, cause distortion of the shape of the concentration-distance curve. Figure 5 presents a theoretical distribution curve of a diffusing impurity in the case of the classical diffusion mechanism and the blackening-density curve which would be obtained by scanning a sample with such a concentration profile, if the diffusate was labeled with the ^{14}C isotope and the sample

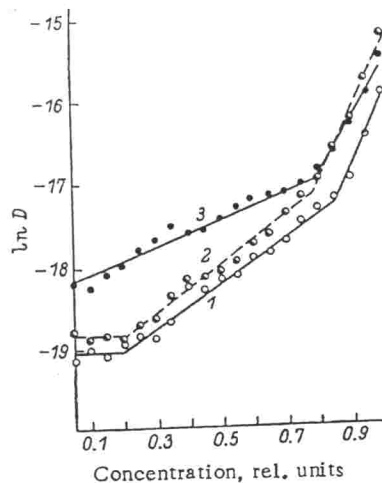


Fig. 7. Dependence of the diffusion coefficient on the concentration of organic solvents in polyethylene: 1) cyclohexane; 2) carbon tetrachloride; 3) benzene.

was made from polyethylene. It is seen that the shape of the photometric curve does not correspond to the shape of the curve for the concentration profile. For this reason we developed a method for restoring the true form of the concentration profile based on the solution of a Fredholm-type integral equation of the first kind

$$I = \int_{-\infty}^{\infty} C(\xi) K(x - \xi) d\xi, \quad (11)$$

where I is the blackening density at a certain point, $C(\xi)$ is the true concentration profile, and $K(x - \xi)$ is the kernel of the Fredholm equation. The function $K(x - \xi)$ can be determined experimentally, since it is equivalent to the photometric curve of an autoradiograph from an infinitely thin layer of the isotope, which is embedded in a polymer block and oriented perpendicularly to the layer of the photographic emulsion. Equation (11) was solved according to the program in [11]. Sufficiently good results on the reconstruction of photometric curves were obtained in model examples with various error levels and widths of the kernel. It should however, be noted that the proposed method works well only when the width of the concentration profile $C(x)$ is several times greater than the width of the function $K(x - \xi)$. In the cases in which the width of the kernel is comparable to $C(x)$, pulsations, which are impossible to eliminate, appear in the solution (Fig. 6). Therefore, the diffusion time must be selected sufficiently large for the effect just indicated to be suppressed.

The treatment of the results of the experiment according to the longitudinal-section method was carried out with the aid of a package of programs which are realized on computers of the BESM-6 type. The package includes a program for smoothing with cubic splines, a program for reconstructing the autoradiograph based on the solution of integral equations, programs for initial evaluation of the diffusion parameters (with the use of the linearization method in [12]), and programs for the calculation of the concentration dependence of the diffusion coefficient.

Figure 7 presents plots of the concentration dependence of the diffusion coefficient calculated from experimental data for cyclohexane, carbon tetrachloride, and benzene in low-density polyethylene. It was found that the dependence can be divided into three sections in all the systems studied: At low diffusate concentrations the diffusion coefficient is practically constant; then, as the concentration is increased, an exponential increase in the diffusion coefficient according to the law $D = D(0)\exp(\beta C)$ begins; and at a concentration greater than 70% of the maximum concentration corresponding to the solubility of the particular diffusate in low-density polyethylene, a sharp increase in D begins. As a result, the diffusion coefficient increases by 1.5-2 orders of magnitude. The value of $D(0)$ increases along the series cyclohexane, carbon tetrachloride, benzene, which is consistent with the dimensions of these molecules. The relative increase is maximal for carbon tetrachloride, and this attests to the strong plasticizing effect of this substance on low-density polyethylene.

In order to refine the value of the diffusion coefficient corresponding to C_{max} , we carried out direct experiments, in which the sorption of the radioactive diffusate occurred in a sample preliminarily saturated with the corresponding inactive substance. In this case, the distribution of the concentration coincides well with the theoretical distribution for the case of a constant D ; however, the values of the diffusion coefficients were approximately 30% higher than the corresponding values determined in the preceding experiments. This is also consistent with the mathematical experiments (Fig. 4B), from which it is seen that the calculation of the concentration dependence from the concentration distribution curve in the sample according to the Matano-Boltzmann method yields somewhat underestimated values at the points corresponding to the maximum concentration.

LITERATURE CITED

1. J. Crank, *The Mathematics of Diffusion*, Oxford University Press (1956).
2. P. V. Danckwerts, *Trans. Faraday Soc.*, 47, No. 8, 1014 (1951).
3. P. V. Danckwerts, *Trans. Faraday Soc.*, 46, No. 4, 300 (1950).
4. H. Gans, *Z. Naturforsch.*, 20a, 298 (1965).
5. F. Van der Maesen and J. A. Brenkman, *J. Electrochem. Soc.*, 102, 229 (1955).
6. B. I. Boltaks, *Diffusion in Semiconductors* [in Russian], *Izd. Fiz.-Mat. Lit.*, Moscow (1961), p. 60.
7. A. Kolodny and J. Shappir, *J. Electrochem. Soc.*, 125, 1530 (1978).
8. C. Van Opdorp, *J. Electrochem. Soc.*, 128, No. 2, 349 (1981).
9. C. Matano, *Jpn. J. Phys.*, 8, 109 (1933).
10. A. Ya. Malkin and A. E. Chalykh, *Diffusion and Viscosity of Polymers. Measurement Methods* [in Russian], *Khimiya*, Moscow (1979).
11. M. V. Aref'eva, in: *Numerical Analysis in FORTRAN. Methods and Algorithms* [in Russian], *MGU*, Moscow (1978), p. 3.
12. T. Dosdale and A. P. Morris, *Philos. Mag.*, A, 42, No. 3, 369 (1980).